Evaluation of edge-induced streaking artifacts in CT scanners

William T. Sheridan, Mark R. Keller, Christopher M. O'Connor, and Rodney A. Brooks

Neuroradiology and Computed Tomography Section, Building 10, Room 11N242, National Institute of Health, Bethesda, Maryland 20205

Kenneth M. Hanson

Los Alamos Scientific Laboratory, Los Alamos, New Mexico 87544

(Received 13 August 1979; accepted for publication 1 November 1979)

A phantom is presented which permits the evaluation of streaking artifacts produced in CT reconstructions by abrupt edges. Its application is demonstrated by results obtained from nine CT scanners. It is observed that even in regions where streaking is not readily apparent, edge-induced artifacts can significantly increase the variance in the reconstruction.

Editor's Keywords: streaking artifacts, phantom, scanner evaluation

I. INTRODUCTION

Since the introduction of the first computed tomography (CT) scanner in 1973, there has been much activity in the development of test objects, or phantoms, for the evaluation of CT image quality.[1-7] These phantoms have almost exclusively focused on basic imaging parameters such as uniformity, slice sensitivity profile, spatial resolution, noise, low contrast detectability, etc. As the state of the art progressed, it became apparent that CT reconstructions were plagued by artifacts of several kinds. In one specific type of artifact, sharp and irregular edges or protuberances of the skull produce streaks across the image that seriously degrade image quality. Figure 1 shows a patient scan where a bony protuberance in the frontal sinus has generated a strong streak pattern radiating downward. Even when these streak patterns are not noticeable due to other image noise, they may still be present and make their own contribution to the effective noise. Such edge-induced streaks can have numerous origins, including mathematical imperfections in the reconstruction algorithm[8,9] as well as physical causes (detector hysteresis, misalignment, etc.).

Unfortunately, no previously described phantom has provided a suitable systematic and quantitative method for evaluating these artifacts. Even the AAPM phantom[1] has only a smooth teflon ring to simulate the skull, and this will not produce streaking effects inside the skull. In this paper, we describe a simple phantom for the evaluation of streaks caused by sharp edges, and report the results obtained on nine current CT scanners. The phantom purposely avoids "shadow" artifacts which arise from beam hardening[10] or from the non-linear partial volume effect[11] and are not edge-related.

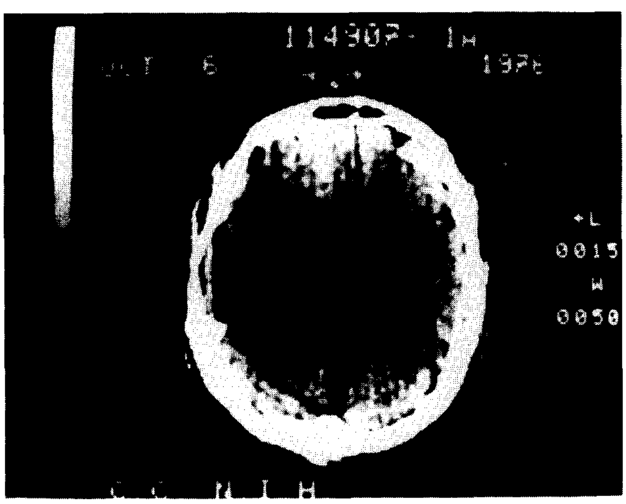

FIG. 1. An actual patient scan with a heavy streak pattern from sharp bone edges and air cavity.

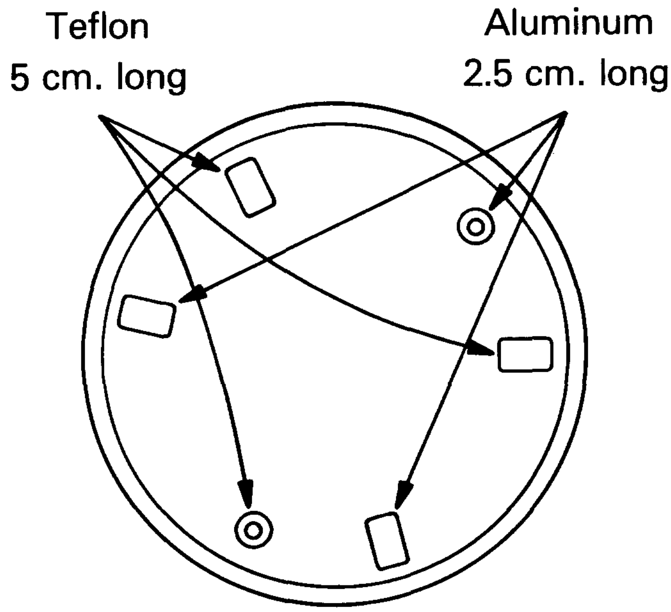

FIG. 2. Diagram of phantom.

II. METHOD

A. Phantom

The design of the phantom is based on the fact that streaks generated by sharp edges are always tangential to the edge, and are most noticeable when the edges are located near the periphery of the reconstruction region. These observations suggested that a group of pins or rods located on the periphery of a uniform phantom will be most suitable for challenging the CT scanners.

After a number of experiments with pins of different sizes, shapes, and materials, the arrangement shown in Fig. 2 proved to be the most suitable. The phantom is contained in

TABLE I. CT scanners used in the present study.

Scanner	Location
Elscint 700	Good Samaritan Hospital, Suffern, NY
EMI CT1010	NINCDS, Clinical Center, National Institutes of Health, Bethesda, MD
EMI CT5005	Clinical Center, National Institutes of Health, Bethesda, MD
GE 8800	Naval Medical Center, Bethesda, MD
Ohio Nuclear Δ2020	Greater Baltimore Medical Center, Baltimore, MD
Pfizer 0200FS	Pfizer Medical Systems, Columbia, MD
Pfizer AS&E	Johns Hopkins, Baltimore, MD
Philips Tomoscan 200	Associated Radiology, NYU School of Medicine, NY
Siemens Somatom	Mercy Hospital, Pittsburgh, PA

a 21-cm outside diameter plexiglass cylinder, 7.6 cm long, filled with water. The phantom is divided into three levels. The first level contains no pins, so that the variance of the CT values in water can be obtained as a reference. The next level includes three teflon pins. These pins, 5 cm long, are attached to the back plate of the box, equally spaced on a concentric 16.5 cm diam circle. Two of them are rectangular with dimensions 1.3 × 0.7 cm, and the other is a 1.1-cm-diam rod with a 0.6-cm hole drilled down the middle. These shapes and arrangements are designed to be a simplified and stylized representation of a challenging human cranial anatomy: the two rectangular pins represent petrous ridges, and the rod with a hole represents a frontal sinus.

In order to create a more difficult challenge, the third level contains in addition a set of three 2.5-cm-long aluminum pins with similar cross section. By incrementing the patient feed a second time, all six pins appear in the field of view.

B. Test procedure

The use of the phantom will be illustrated with results obtained from the nine commercial CT scanners listed in Table I. In each case, the scanner was not specifically prepared for the test but was used in the same manner as routine patient head scans. The phantom was usually supported by a head rest. After careful positioning of the phantom, scans were made at the three levels described above.

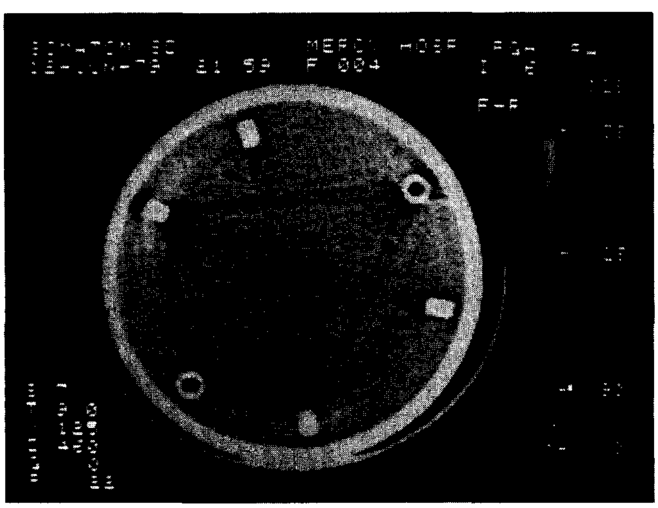

FIG. 3. Scan of aluminum and teflon pins taken with Siemens Somatom.

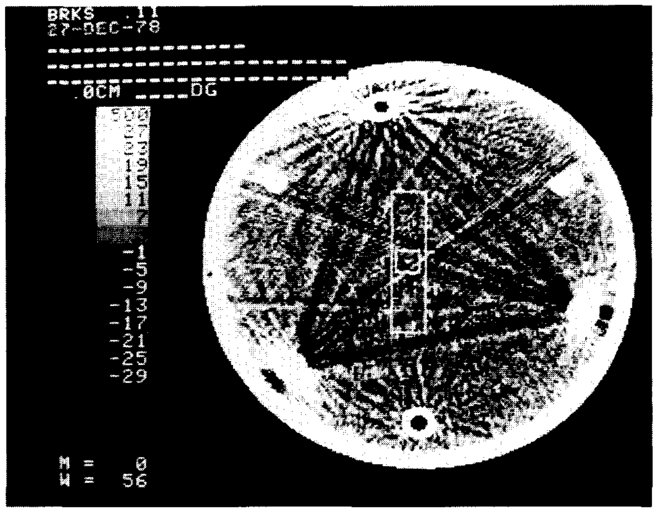

FIG. 4. Scan of aluminum and teflon pins taken with Pfizer 0200FS.

C. Data analysis

The increase in the variance near the center of the reconstruction produced by the pins provides a quantitative measure of the edge-induced streaking artifacts. By placing the area of interest at the center, shadow artifacts which fall between pins are largely avoided. The net variance arising from statistically independent sources of fluctuations is simply the sum of the variances for the individual contributions. Thus, the difference between the variance in level 2 (σ_2^2) and that in level 1 (σ_1^2), $\sigma_2^2 - \sigma_1^2$, represents the variance arising from the artifacts produced by the teflon pins. Similarly, $\sigma_3^2 - \sigma_2^2$, represents the variance produced by the aluminum pins. Note that the variances at all three levels have contributions from x-ray counting statistics and should diminish as the dose is increased. However, the differences $\sigma_2^2 - \sigma_1^2$ and $\sigma_3^2 - \sigma_2^2$, should be independent of the dose. The

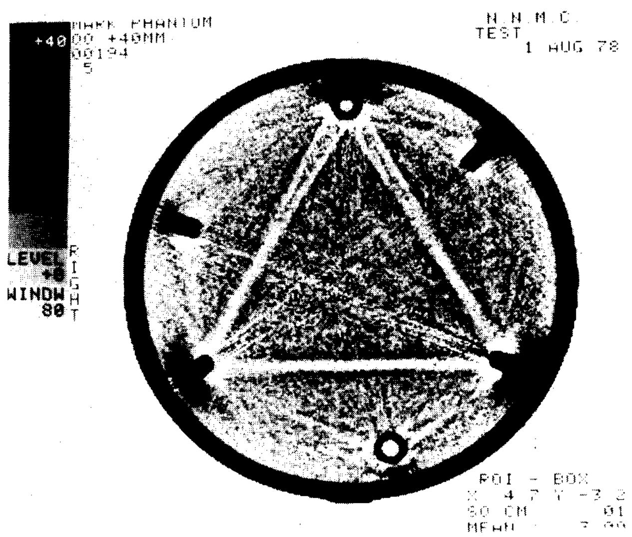

FIG. 5. Scan of aluminum and Teflon pins taken with GE 8800.

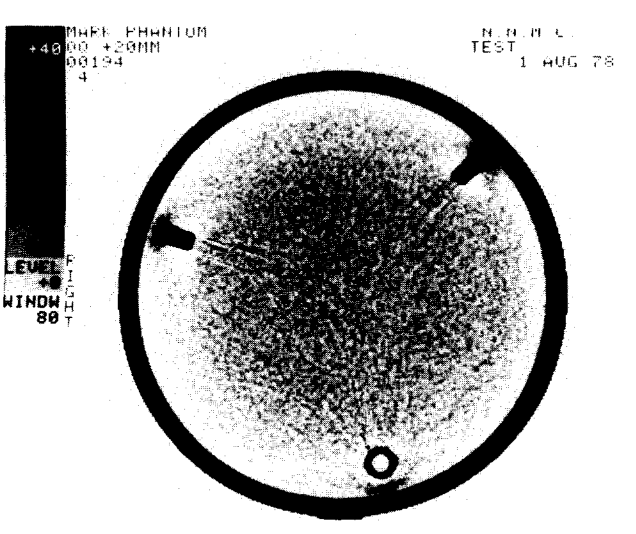

FIG. 6. Scan of teflon pins taken with GE 8800.

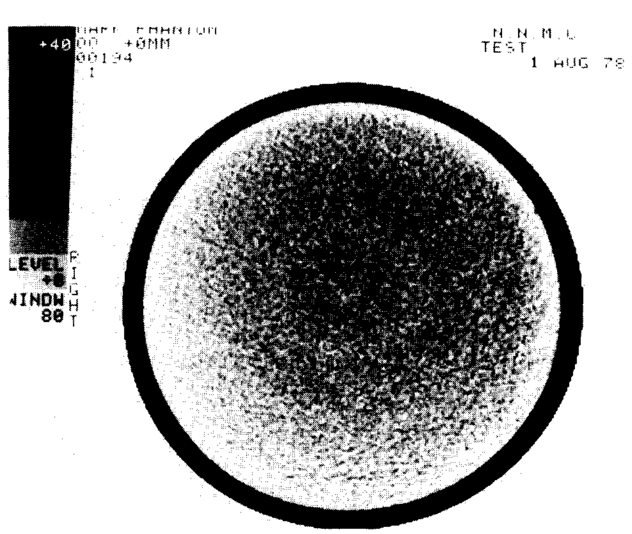

FIG. 7. Water scan taken with GE 8800.

variances were found on several scanners to be fairly insensitive to the size of the areas used in the variance calculation. Several of the scanners used in this study had no "area of interest" calculational option so the results had to be calculated from pixel-by-pixel printout. To avoid excessive hand calculation, the results quoted below are for either a 1- × 1-cm square or a 1-cm-diam circle.

The statistical uncertainty in the results is not insignificant and must be considered. The standard deviation in the difference of the variance ($\sigma_2^2 - \sigma_1^2$) is crudely estimated to be

$$[4(\sigma_1^4 + \sigma_2^4)/N]^{1/2},$$

where N is the number of pixels used in each variance calculation. This expression is based on the standard deviation of the variance for uncorrelated Gaussian noise.[12] It ignores the effect of the long-range negative correlations known to exist in the statistical noise found in CT.[13] It is assumed that the number of independent noise samples is half the number of pixels used. This has been approximately verified for the EMI 5005 scanner.[13] This assumption depends upon the filter function used in the CT reconstruction algorithm. While the filter function is not known for other scanners, the above assumption is probably not seriously in error. If the filtering is less extreme, then the statistical uncertainty in the result is reduced from our tabulated value.

III. RESULTS

Figures 3–7 present a sampling of the CT images obtained in this study. Many of the pin scans had readily apparent streaking artifacts, particularly near the pins themselves. The results of the data analysis described above are presented in Table II. Some of the scanners showed statistically significant increases in the variance near the center of the phantom for the teflon pins. All but one showed significant increases for the aluminum pins. It is expected from the relative linear attenuation coefficients of water, teflon, and aluminum in the effective x-ray energy region around 70 keV that the ratio of the increase in variance for the aluminum pins to that for the teflon pins should be toughly 5:1. The data in Table II are consistent with this ratio within the often large uncertainties quoted.

It is interesting to note that in most cases the increase in variance arising from the teflon pins is comparable to the intrinsic variance of the water bath (σ_1^2). Thus, it is likely that edge-induced artifacts have an effect on the detection capabilities for low-contrast lesions.[14,15]

The results listed in Table II are intended to illustrate the use of the edge-induced artifact phantom presented here and to demonstrate that edge-induced artifacts are indeed important in many present-day commercial scanners. These results should not be used for comparative purposes at this

TABLE II. Summary of variances measured with streak artifact phantom. The contribution to the variance from the teflon pins ($\sigma_2^2 - \sigma_1^2$) and its estimated statistical uncertainty (one standard deviation) is given as well as the same for the aluminum pins ($\sigma_3^2 - \sigma_2^2$). The units of the variances quoted are (CT numbers)^2 using 1000 CT numbers as the water-air difference.

Scanner	Pixel size (mm)	Number of pixels used	σ_1^2 (water)	$\sigma_2^2 - \sigma_1^2$	$\sigma_3^2 - \sigma_2^2$
Elscint 700	1.0	100	9	0 ± 6	16 ± 8
EMI CT1010	1.5	37	8.8	15 ± 8	110 ± 45
EMI CT5005	1.5	49	19	12 ± 10	5 ± 13
GE 8800	0.8	100	4.8	7.2 ± 2.6	30 ± 9
Ohio Nuclear Δ2020	0.49	169	155	22 ± 36	15 ± 40
Pfizer AS&E	0.50	200	39	20 ± 10	19 ± 14
Pfizer 0200FS	1.0	100	4	37 ± 18	88 ± 37
Siemens Somatom	1.1	81	3.8	3.4 ± 1.8	5.9 ± 3.4
Philips Tomoscan 200	0.97	100	32	12 ± 11	66 ± 24

time as CT manufacturers are continually implementing improvements on scanners in the field.

IV. DISCUSSION

The frequency characteristics of edge-induced artifacts have not been explored in this study. However, since these artifacts are induced by sharp edges, it is expected that they are chiefly composed of high frequency components. Thus, we would expect that the magnitude of the edge-induced artifacts be strongly influenced by the spatial resolution through the choice of the reconstruction filter function. Further, these artifacts may be related to pixel size through its effect on aliasing.[9]

It might be argued that the increase in noise variance near the center of the reconstruction may arise from the detection of fewer x rays due to increased absorption of the x rays by the pins. This effect is negligible: the decrease in the number of noise equivalent quanta (NEQ)[15,16] near the center of the phantom is calculated to be less than 4% for level 3 (aluminum plus teflon pins). Thus the increase in variance should be less than 4% on this account.

It will be noted that prominent shadows occur between the aluminum pins in Figs. 3–5. These bands are undoubtedly produced by non-linear, beam hardening effects.[10] This effect probably occurs between the teflon and aluminum pins although it should be quite small. Thus, the phantom used in this study could be improved by eliminating the teflon pins from the aluminum pin level.

The data analysis employed in this study might be better performed in the future by using larger areas for the calculation of the variances, e.g., 3×3 cm, in order to reduce statistical uncertainties.

ACKNOWLEDGMENTS

We wish to thank the institutions listed in Table I for their cooperation in obtaining the CT scans reported in this work. One of the authors (K.M.H.) acknowledges the support of the U.S. Department of Energy.

[1]P. F. Judy, S. Balter, D. Bassano, E. C. McCullough, M. T. Payne, and L. Rothenberg, Report No. 1, "Phantoms for Performance Evaluation and Quality Assurance of CT scanners," (AAPM, Chicago 1977).
[2]A. J. Duerinckx and A. Macovski, J. Comput. Assist. Tomogr. **2**, 481 (1978).
[3]L. M. Zatz, J. Comput. Assist. Tomogr. **2**, 336 (1978).
[4]E. C. McCullough, J. T. Payne, H. L. Baker, Jr., R. R. Hattery, P. F. Sheedy, D. H. Stephens, and E. Gegaudus, Radiology **120**, 173 (1976).
[5]D. J. Goodenough, K. E. Weaver, and D. O. Davis, Opt. Eng. **16**, 52 (1977).
[6]M. Endo, E. Takenaka, T. Iinuma, Y. Tateno, and Y. Suda, Nippon Igaku Hoshasen Gakkai Zasshi **38**, 33 (1978).
[7]C. M. Bellon, F. D. Miraldi, and E. J. Wiesen, Appl. Radiol. **8**, 53 (1979).
[8]R. A. Brooks, G. H. Weiss, and A. J. Talbert, J. Comput. Assist. Tomogr. **2**, 557 (1978).
[9]R. A. Brooks, G. H. Glover, A. J. Talbert, R. L. Eisner, and F. A. DiBianca, J. Comput. Assist. Tomogr. **3**, 511 (1979).
[10]P. M. Joseph and R. D. Spital, J. Comput. Assist. Tomogr. **2**, 100 (1978).
[11]G. H. Glover and N. J. Pelc, J. Comput. Assist. Tomogr. **3**, 573 (1979).
[12]J. B. Kennedy and A. M. Neville, *Basic Statistical Methods for Engineers and Scientists*, 2nd ed. (Thomas Y. Crowell, New York 1976), p. 239.
[13]K. M. Hanson and D. P. Boyd, IEEE Trans. Nucl. Sci. **NS-25**, 160 (1978).
[14]K. M. Hanson, Proc. SPIE, Appl. Opt. Instrum. Med. VI, **127**, 304 (1977).
[15]K. M. Hanson, Med. Phys. **6**, 441 (1979).
[16]R. F. Wagner, D. G. Brown, and M. Pastel, Med. Phys. **6**, 83 (1979).

ANNOUNCEMENT

Radiation Biology pre-doctoral traineeships and post-doctoral fellowships, emphasizing research training and experience, available at Colorado State University, Fort Collins, Colorado.

Candidates should submit applications by April 14, 1980, for positions that start in September. For further information, write:

Dr. J. S. Bedford
Department of Radiation Biology
Colorado State University
Fort Collins, CO 80523.